AD-A160 705 LARGE-AREA SHORT-PULSE SURFACE DISCHARGES FOR LASER EXCITATION(U) BEVERLY (R E) III AND ASSOCIATES COLUMBUS OH* R E BEVERLY 1984 ARO-22480.2-PH DAAG29-84-C-0027 1/1

UNCLASSIFIED F/G 20/3 NL

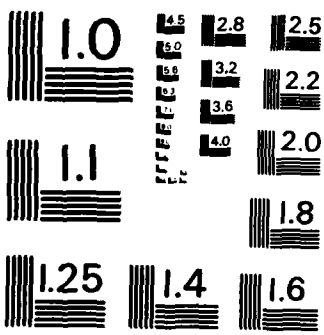

UNCLASSIFIED
SECURITY CLASSIFICATION OF THIS PAGE (When Data Entered)

(2)

REPORT DOCUMENTATION PAGE

READ INSTRUCTIONS BEFORE COMPLETING FORM

1. REPORT NUMBER: ARO 22480.2-PH
2. GOVT ACCESSION NO.: N/A
3. RECIPIENT'S CATALOG NUMBER: N/A

4. TITLE (and Subtitle): Large-Area Short-Pulse Surface Discharges for Laser Excitation

5. TYPE OF REPORT & PERIOD COVERED: Conference Proceedings 1 Oct 1984-1 Nov 1984

6. PERFORMING ORG. REPORT NUMBER:

7. AUTHOR(s): R. E. Beverly III

8. CONTRACT OR GRANT NUMBER(s): DAAG29-84-C-0027

9. PERFORMING ORGANIZATION NAME AND ADDRESS:
R. E. Beverly III and Associates
1891 Fishinger Road
Columbus, OH 43221

10. PROGRAM ELEMENT, PROJECT, TASK AREA & WORK UNIT NUMBERS: 22480-PH

11. CONTROLLING OFFICE NAME AND ADDRESS:
U. S. Army Research Office
Post Office Box 12211
Research Triangle Park, NC 27709

12. REPORT DATE:

13. NUMBER OF PAGES:

14. MONITORING AGENCY NAME & ADDRESS (if different from Controlling Office):

15. SECURITY CLASS. (of this report): Unclassified

15a. DECLASSIFICATION/DOWNGRADING SCHEDULE:

16. DISTRIBUTION STATEMENT (of this Report)

Approved for public release; distribution unlimited.

17. DISTRIBUTION STATEMENT (of the abstract entered in Block 20, if different from Report)

NA

18. SUPPLEMENTARY NOTES

The view, opinions, and/or findings contained in this report are those of the author(s) and should not be construed as an official Department of the Army position, policy, or decision, unless so designated by other documentation.

19. KEY WORDS (Continue on reverse side if necessary and identify by block number)

Surface discharges
Ultraviolet optical sources
Radiative properties
Electrical properties
Spatial homogeneity
Preionization of laser media
Photoinitiation of laser media
Photodissociation of laser media

20. ABSTRACT (Continue on reverse side if necessary and identify by block number)

Large-area (100-400 cm^2), short-pulse (~1 μsec) planar surface discharges were produced across various polymer dielectric substrates and in several gas environments at pressures up to several atmospheres. The dependence of radiative behavior upon electrical driver parameters was investigated and criteria for obtaining spatially homogeneous, coalesced discharges were developed. Applications for excitation of laser media are reviewed.

DD FORM 1 JAN 73 1473 EDITION OF 1 NOV 65 IS OBSOLETE

UNCLASSIFIED
SECURITY CLASSIFICATION OF THIS PAGE (When Data Entered)

Proceedings International Conference on LASERS 84
(San Francisco, California USA, 26-30 November, 1984)

LARGE-AREA SHORT-PULSE SURFACE DISCHARGES FOR LASER EXCITATION*

R. E. Beverly III
R. E. BEVERLY III AND ASSOCIATES
1891 Fishinger Road
Columbus, Ohio 43221
USA

Abstract

Large-area (100-400 cm^2), short-pulse (~1 μsec) planar discharges employing profiled electrodes have been produced across various polymer substrates, including polyethylene, polyethylene terephthalate, cellulose acetate, polytetrafluoroethylene, and fiberglass. All discharges were complete (i.e., completely bridged the anode-cathode gap) and operated in the moderate erosion regime ($E_d/A \sim 1$ J/cm^2). Parametric studies of the electrical circuit parameters and discharge dimensions demonstrate the importance of proper source-driver impedance matching to short-pulse operation. The degree of spatial homogeneity depends upon the peak discharge voltage, the initial rate of voltage rise, the specific capacitance of the substrate, the gas atmosphere and pressure, and the ablation mode of the substrate. Open-shutter photography, performed both perpendicular and parallel to the discharge plane, is used to develop criteria for obtaining uniform, coalesced discharges. Spectroscopic studies show that planar surface discharges radiate as Lambertian sources characterized by brightness temperatures > 30,000 K. The plasma is not opaque in the ultraviolet and shows considerable structure attributed to line emission. Coupling schemes for interfacing surface discharges to gaseous laser media in various geometries have been developed.

Introduction

Surface discharges offer numerous advantages as an ultraviolet source for lasers.[1] Some of these advantages include intense, short-pulsewidth emission which can be tailored for enhanced radiation in the spectral region of interest, scalability to large planar or cylindrical areas which are suitable for close-coupled excitation, life expectancies which can be extended to 10^6 flashes with proper engineering, simple and inexpensive designs which can withstand high-peak-power electrical loading without catastrophic failure, and capability for repetitively pulsed operation.

The primary emphasis of the present experiments is on spectroscopic and electrical characterization of the discharges over a range of source and driver parameters. The geometry of the planar source and an equivalent circuit schematic are shown in Fig. 1. The discharge width and gap are given by w and d, respectively, and the source area is A. Experiments have been performed both with Chang[2] profile and parallel electrodes of various widths. The electrode material is brass. The main energy storage capacitor C_s is charged to a voltage V_c (stored energy $E_s = 0.5C_sV_c^2$) and is discharged into the load (deposited energy E_d) by two parallel N_2-pressurized spark gaps. Peaking capacitors C_p are used to increase the current and optical rise time at the load. The total circuit inductance is $L = L_0 + L_1$. Current waveforms are measured using an Ion Physics Company Model CM-1-S current monitor, while voltage waveforms are measured using a custom-built coaxial divider.

The optical diagnostics system and overall experimental arrangement are shown by the plan view in Fig. 2. A Tracor-Northern Diode Array Rapid Scan Spectrometer (DARSS) is used to obtain time-integrated quantitative spectra. The intensified diode array detector contains 1024 elements and can span 40 nm or 300 nm in a single exposure depending upon which grating is employed in the Ebert spectrometer. Wavelength calibration of the DARSS system is performed using a low pressure Hg-Ar arc lamp. The optical transfer system, spectrometer, and DARSS were calibrated as a system using an NBS-traceable standard of spectral radiance. Two photomultiplier (Hamamatsu R-1509) assemblies are used to measure temporal dependencies. Assembly #1 is used in conjunction with various bandpass filter/pinhole aperture arrangements to measure optical pulse shapes, while assembly #2 is used to follow the temporal evolution of line species in the discharge. Data from the DARSS mainframe is downloaded to a PDP-11/23 computer for analysis and plotting. Signals from the PMTs, current, and voltage monitors are recorded using a TEK 7704A oscilloscope.

*Research supported in part by the U. S. Army Research Office under Contract Number DAAG29-84-C-0027.

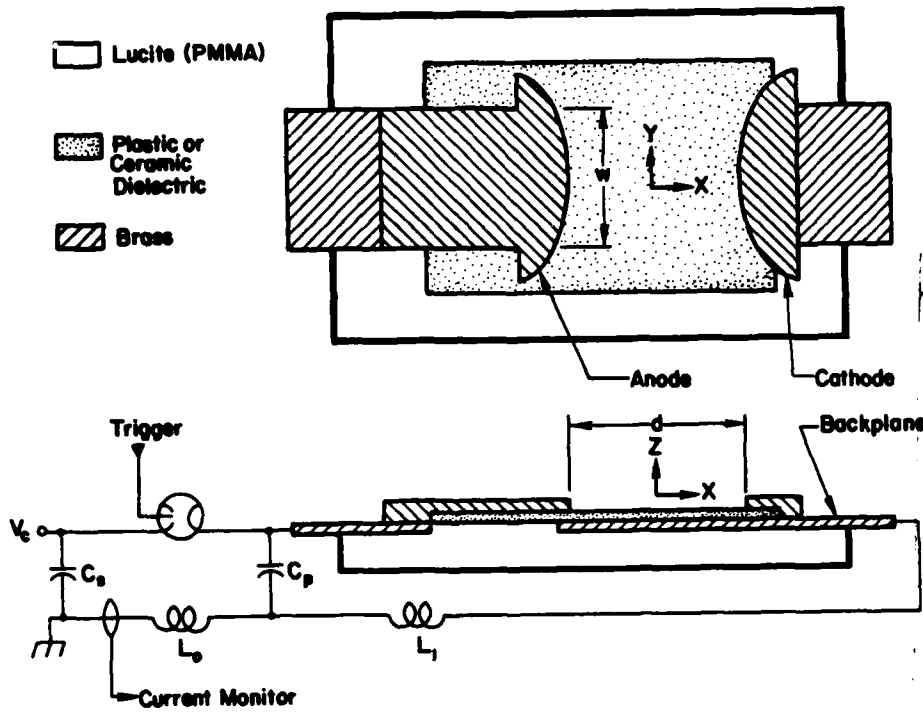

Fig. 1. Planar surface-discharge source and equivalent circuit.

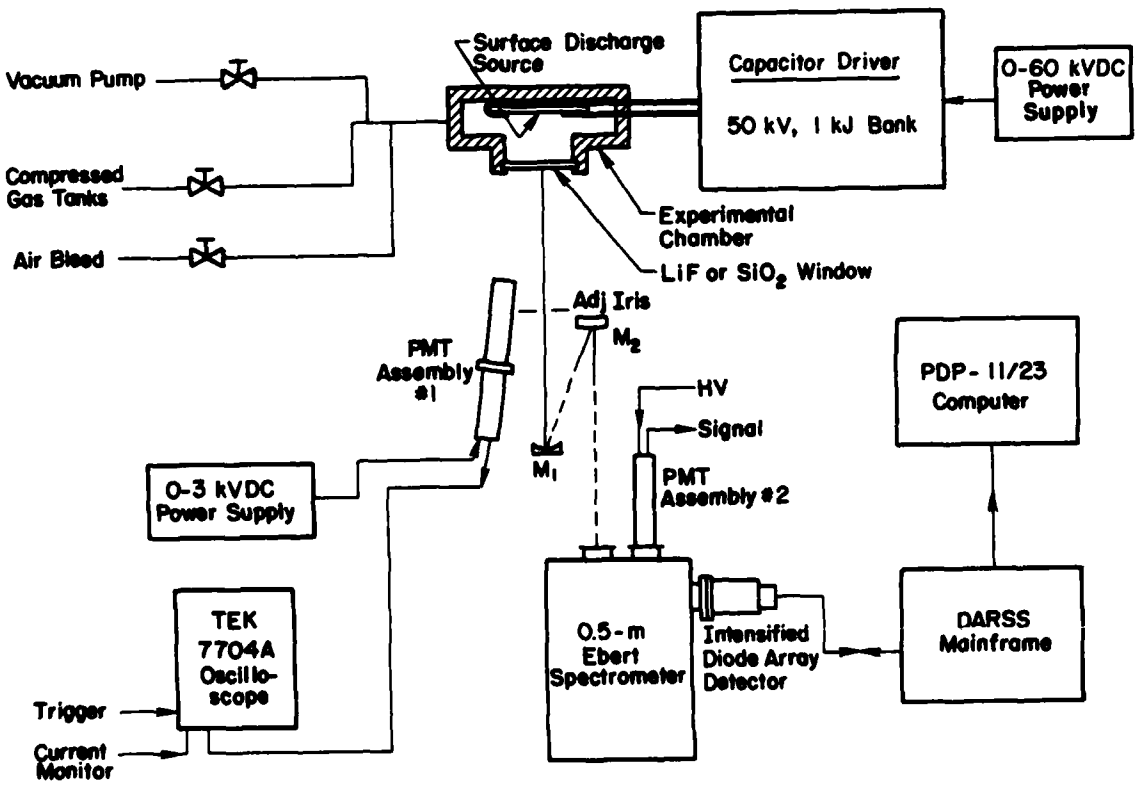

Fig. 2. Optical diagnostics system and experimental arrangement.

Electrical Properties

Surface discharges are inherently low-impedance (< 1Ω) loads. The condition for critical damping of the current waveform, $Z_d = 0.5Z_s$, where Z_d and Z_s are the driver and source impedance, respectively, is also the condition required to maximize the power into the source load. For a purely reactive driver, $Z_d = \sqrt{L/C}$, requiring low-inductance circuitry for short optical pulsewidths. Current waveforms for all the experiments reported here are oscillatory or near-critically damped. The peak current, I_p, shows little or no dependence on the gas type, gas pressure, or dielectric chosen. As shown in Fig. 3, $I_p \propto V_c\sqrt{C_s/L}$, as is expected from elementary circuit analysis. The time at which the peak current is reached decreases and $dI/dt|_0$ increases with increasing C_p. Preliminary data suggest that the source resistance increases directly with the gap d, for $d >> d_s$, where d_s is the characteristic electrode sheath dimension. The source resistance is not directly proportional, however, to the reciprocal of the discharge width, 1/w. For example, the inferred source resistances for w = 10 and 20 cm discharges (d = 11 cm, C_s = 868 nF, L = 284 nH, V_c = 15 kV, 800 Torr Ar) are 135 and 123 mΩ, a decrease of only 10% for a doubling in discharge width. This behavior is probably related to the functional dependence of the magnetic pressure upon the plasma on the current density thru the plasma. More complete parametric studies are presently underway to elucidate this phenomenon. Thus, for a given V_c, d can be increased to a value for which the critical damping requirement is satisfied. Because of the low impedance of the load, the electrical efficiency of the discharge, $\eta = E_d/E_s$, depends sensitively on external losses such as the characteristic loss resistance of the capacitor(s) and the transmission line resistance.[1] Every effort should be made to minimize these losses if the electrical-to-optical conversion efficiency is important.

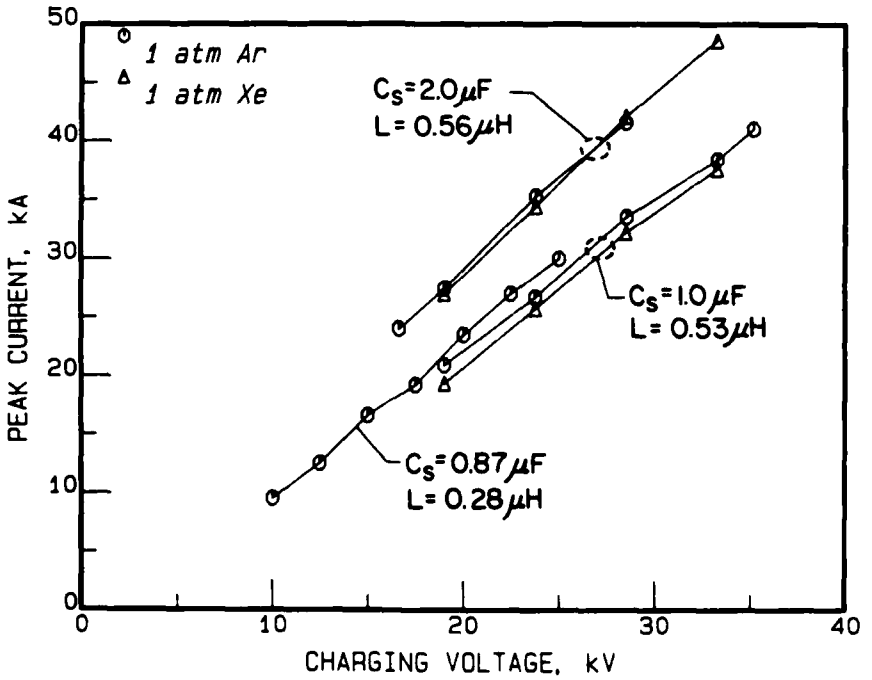

Fig. 3. I_p as a function of V_c. Data for the 1 and 2 μF cases are for 4 x 4 cm^2 discharges across chromium oxide and are taken from the work of Beverly et al.[3] Data for the 868 nF case is for 10 x 11 cm^2 discharges across cellulose acetate.

Radiative Properties

Radiative enhancement in a particular spectral region can be effected by choosing a substrate whose species readily ionize in the discharge plasma and subsequently radiate via line transitions in the region of interest. Beverly et al.[3] investigated numerous ceramics in surface discharges and showed, for example, that significant enhancement in the 350-450 nm region occurs using cerium oxide and strontium titanate substrates. For the plastic substrates employed here, no appreciable differences were noted in the time-integrated spectra when using different plastics and few line species attributed to components of the substrates were observed. DARSS spectra, such as those in Fig. 4, show considerable

structure although most of the lines arise from excited species in the ambient gas atmosphere. Analysis of these spectra shows that the radiated energy density within a given pumpband of width $\Delta\lambda$, $E_{\Delta\lambda}/A$, increases rapidly with increasing absolute gas pressure P, saturating at P = 2-4 atm. Although $E_{\Delta\lambda}/A$ saturates with increasing E_d/A, the radiant excitance $M_{\Delta\lambda} = (E_{\Delta\lambda}/A)/t_p$ continues to increase since there is a tendency for the optical pulsewidth t_p to decrease with increasing V_c. Thus, surface discharges can attain a larger radiant excitance over a much larger area than produced at the surface of a highly-stressed, optimized xenon flashlamp for comparable pulsewidths. Sources in the rare gases yield values of E_{uv} which are proportional to the atomic weight of the gas.

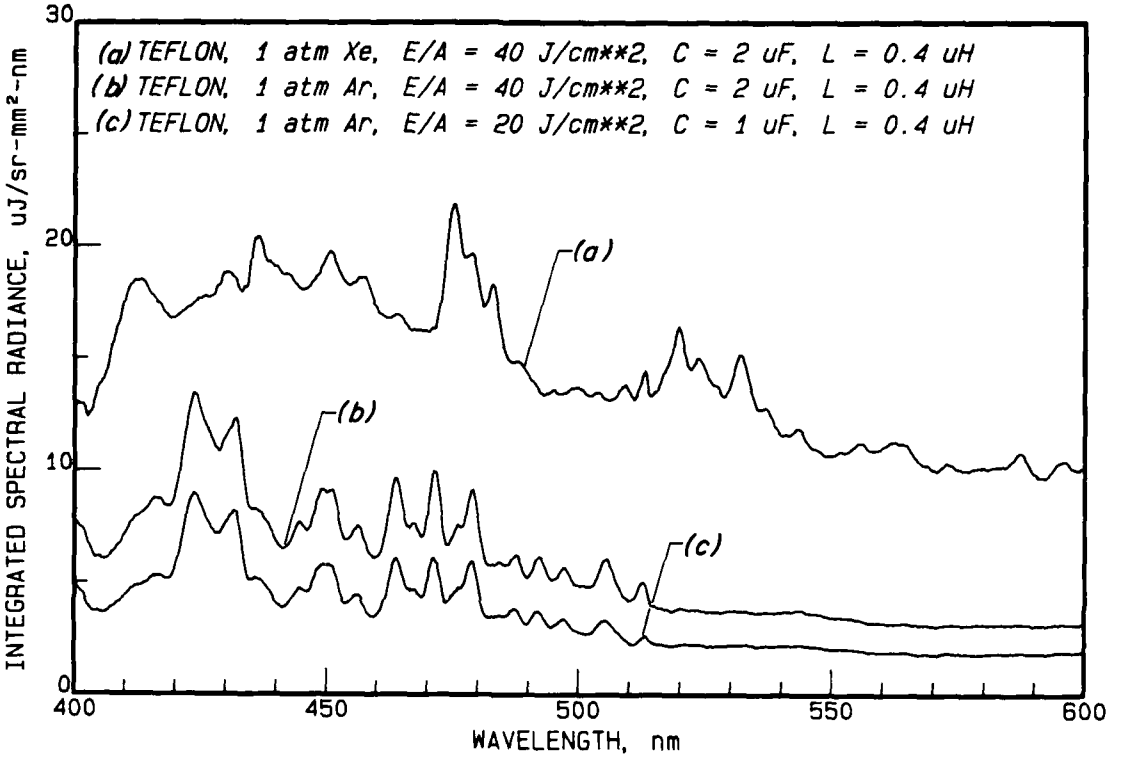

Fig. 4. Representative DARSS spectra.

The optical pulse shape is characterized by a fast leading edge, an optical peak temporally coincident with the current maximum, and a quasi-exponential decay which is a few times longer in duration than the leading edge if the current waveform is damped to as much as 100 times longer for oscillatory discharges. The use of peaking capacitors can therefore be extremely effective in decreasing the optical rise time as well as the pulsewidth. For the case of ceramic substrates, neutral line species are observed to radiate for many tens of microseconds into the afterglow. Singly- and doubly-ionized substrate species, however, tend to turn-on and terminate earlier in the discharge than the neutrals.

Spatial Homogeneity

The degree of spatial homogeneity depends upon the applied voltage (U), the rate of initial voltage rise $(dU/dt|_0)$, the specific capacitance of the substrate [C_{sp} (pF/cm^2) = $0.88\kappa/\Delta$, where κ is the dielectric constant and Δ (mm) is the substrate thickness], the gas atmosphere and pressure, and the ablation mode of the substrate. Complete surface discharges do not obey Paschen's law and, in fact, can be achieved using voltages far lower than required to break down the equivalent free-spark gap. For $U < U_{br}$, where the breakdown voltage U_{br} is a function of C_{sp} and the gas type,[4] the surface discharge is incomplete, consisting of a number of plasma channels which advance nonuniformly and which have a highly chaotic appearance. As the degree of overvoltage (U/U_{br}) is increased, the number of plasma channels increases and the homogeneity improves. For $U/U_{br} > 3$, these channels coalesce into a uniform plasma sheet as shown in Fig. 5. The work of Baranov[5] has shown that the number and width of these plasma channels is also a function of $dU/dt|_0$ for discharges in helium. We have observed similar behavior for discharges in nitrogen and air, which require low-inductance circuitry to achieve homogeneous planar discharges

($dU/dt|_0 \gtrsim 10^{10}$). Planar discharges in the heavy rare gases (xenon, argon, and krypton) are comparatively easy to achieve even at high pressure (10 atm). The effect of increasing gas pressure for discharges in nitrogen is shown in Fig. 6. The number of channels decreases with increasing pressure but their width tends to increase. The presence of an attaching gas, as demonstrated by the photographs in Fig. 7, makes the discharge highly filamentary. At sufficiently high pressure, the discharge will convert from surface tracking to a single arc. It is possible to obtain a multichannel surface discharge in laboratory air for fast discharge circuitry as shown in Fig. 8. The number of channels per unit of discharge width increases with increasing U and decreasing L. The presence of a conducting backplane is absolutely necessary to produce a homogeneous planar discharge as well as to reduce the breakdown voltage. Preliminary results suggest that operating the discharge in the negative polarity mode, i.e. $V_c < 0$, is preferrable to operation in the positive mode. Our experiments show that a minimum value of $C_{sp} = 2\text{-}4$ pF/cm^2 is necessary but not sufficient for homogeneity. Increases in C_{sp} beyond 10 pF/cm^2 show little additional benefit. Increasing C_s with the Chang profile electrodes causes the discharge to widen in the y-direction as shown in Fig. 9. Wide electrodes benefit from distributing the peaking capacitance along their length which helps to prevent plasma formation in only one region. We note that the spatial homogeneity is not especially sensitive to details of the electrode contour, indicating that $d\xi_z/dz >> d\xi_x/dx$ in conformance with the theory of Borisov et al.[6] Here, ξ is the electric field strength. Substrates which ablate cleanly during the discharge (e.g. most plastics, chromium oxide, strontium titanate) display good spatial homogeneity while substrates which metallize during the discharge (e.g. niobium oxide) show progressively degraded homogeneity as flashes are accumulated. This phenomenon is explained by reduction of the ceramic to free metal during the initial discharges followed by single-track breakdown on the surface of the substrate during later flashes.

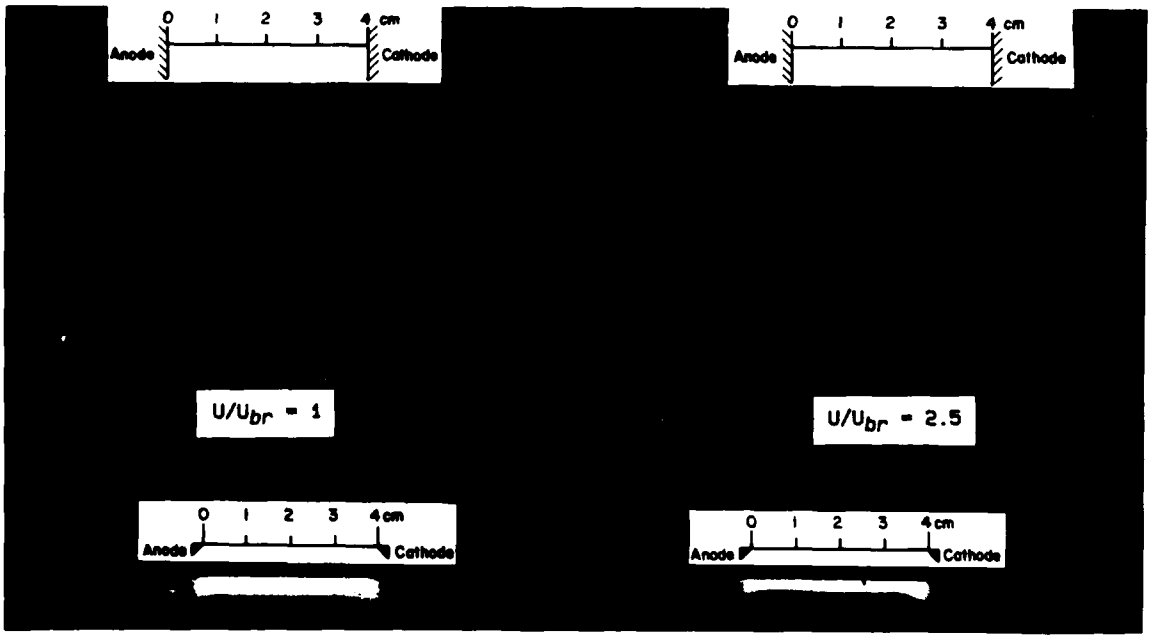

Fig. 5. Effect of increasing degree of overvoltage on spatial homogeneity (chromium oxide dielectric, $C_{sp} = 2.2$ pF/cm^2; parallel electrodes, w x d = 4 x 4 cm^2; 380 Torr argon; $C_s = 1.0$ μF, L = 532 nH).

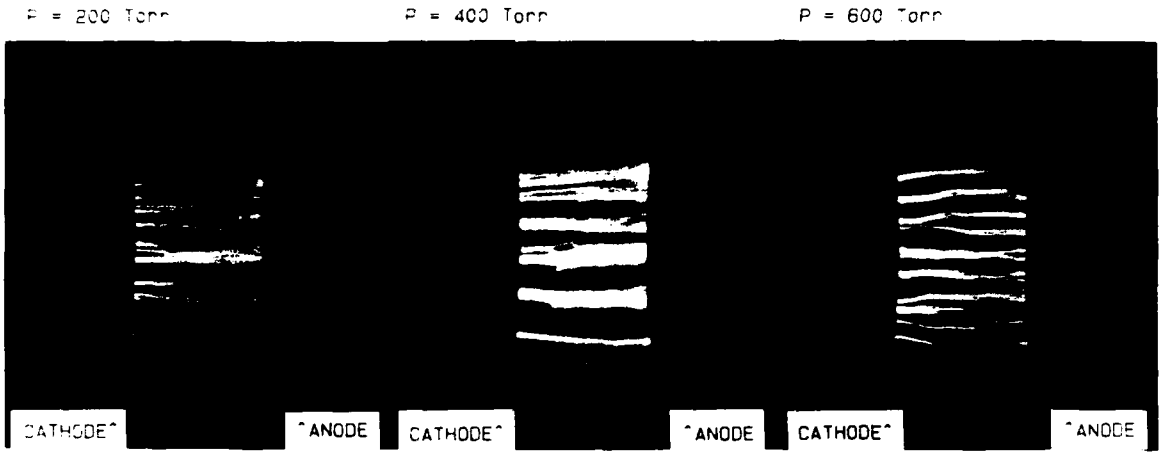

Fig. 6. Effect of increasing gas pressure (nitrogen) on spatial homogeneity (polyethylene terephthalate dielectric, C_{sp} = 11.7 pF/cm^2; Chang profile electrodes, w x d = 20 x 6 cm^2; V_c = 25 kV, C_s = 434 nF, C_p = 6.6 nF, L = 284 nH).

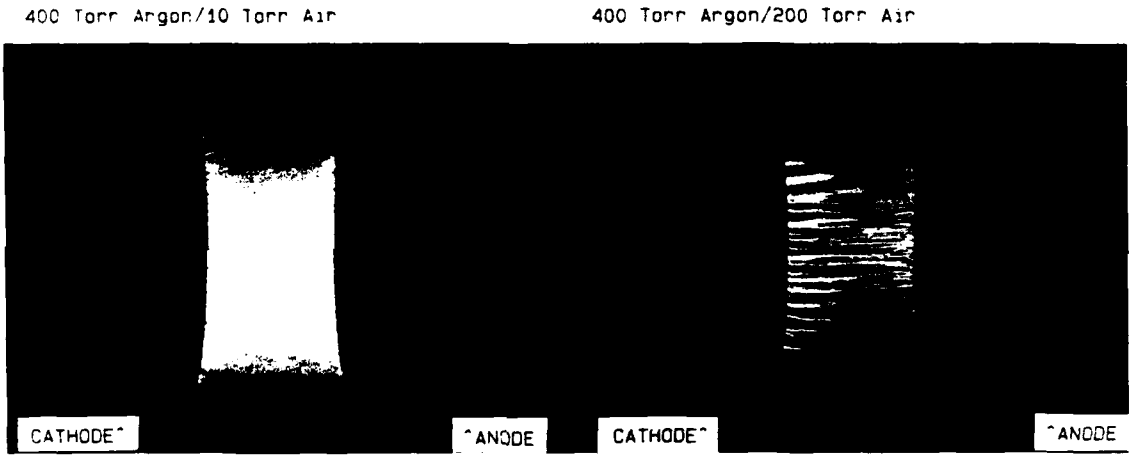

Fig. 7. Effect of an attaching gas on spatial homogeneity (source and electrical parameters same as in Fig. 6).

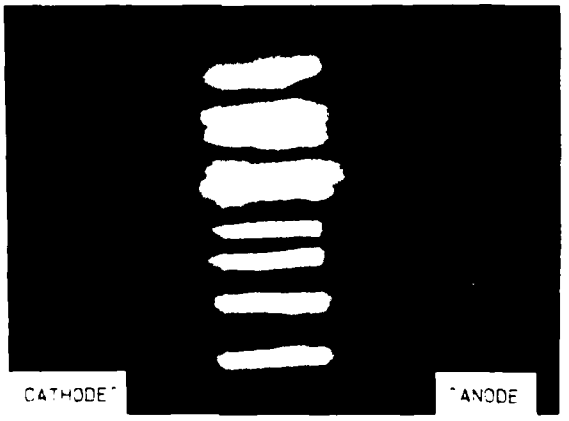

Fig. 8. Fast multichannel surface discharge in laboratory air (glass fiber phenolic dielectric, C_{sp} = 2.8 pF/cm^2; parallel electrodes, w x d = 6 x 2.5 cm^2; V_c = 25 kV, C_s = 868 nF, L = 229 nH).

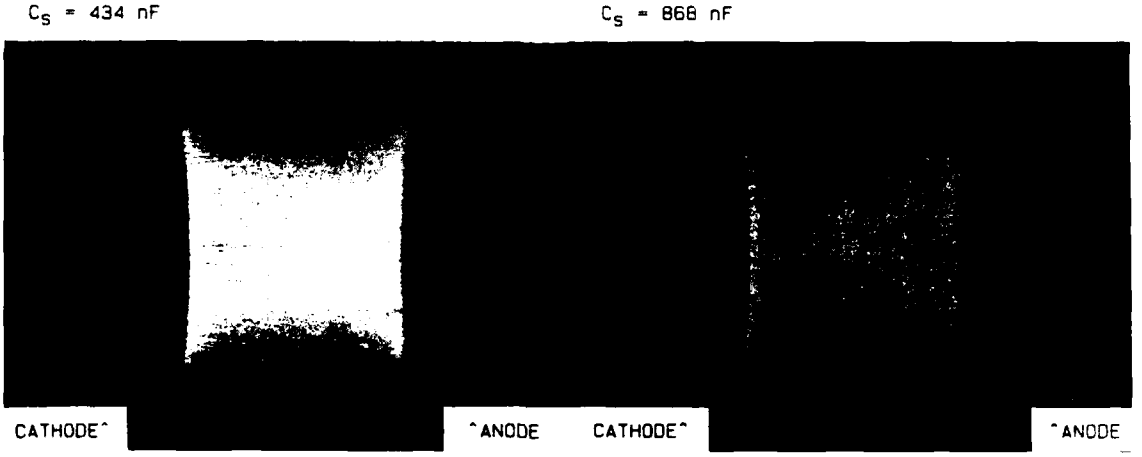

Fig. 9. Effect of energy storage capacitance on spatial homogeneity (fiberglass dielectric, C_{sp} = 3.0 pF/cm^2; Chang profile electrodes, w x d = 20 x 10 cm^2; 800 Torr argon; V_c = 25 kV, C_p = 6.6 nF, L = 284 nH).

Excitation of Laser Media

Surface discharges have been successfully used to pump photodissociation excited media,[7-9] to preionize carbon-dioxide[10-20] and excimer[21-23] lasers, and to photoinitiate HF/DF chemical lasers.[24-30] Engineering considerations for incorporating surface discharge uv sources into repetitively pulsed lasers are given by the present author in Ref. 31. Conceptual pumping geometries are shown in Fig 10. The parallel planar geometry is most suited to large transverse discharge lasers where the surface discharges act as uv-preionizers for the gas and as the plasma electrodes for the main discharge. The inside-out cylindrical and annular schemes are amenable to axial-flow devices with the former being the most compact and the latter affording better scalability. The outside-in cylindrical geometry is of interest for radial-injection chemical lasers.

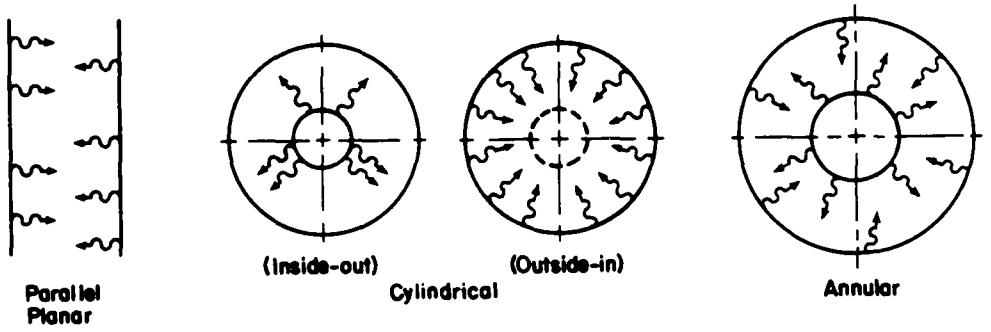

Fig. 10. Surface-discharge pumping geometries.

References

1. R. E. Beverly III, in Progress in Optics, Vol. XVI, ed. E. Wolf (North-Holland, Amsterdam, 1978), pp. 357-411.
2. T. Y. Chang, Rev. Sci. Instrum. 44, 405 (1973).
3. R. E. Beverly III, R. B. Schaefer, D. G. Youmans, and T. W. Hilton, Final Technical Report on Contract DAAH01-83-D-A017 (Work Orders 3 and 4).
4. S. I. Andreev, E. A. Zobov, A. N. Sidorov, and V. D. Kostovsov, J. Appl. Mech. Tech. Phys. 21, 103 (1980).
5. V. Yu. Baranov, V. M. Borisov, F. I. Vysikaylo, Yu. B. Kiryukhin, and O. B. Khristoforov, Preprint IAE-3472/7, I. V. Kurchatov Institute of Atomic Energy (Moscow, 1981).
6. V. M. Borisov, F. I. Vysikaylo, and O. B. Khristoforov, High Temp. 21, 635 (1983) [Teplofiz. Vys. Temp. 21, 844 (1983)].

7. R. E. Beverly III, R. H. Barnes, C. E. Moeller, and M. C. Wong, Appl. Opt. 16, 1572 (1977).
8. I. M. Belousova, O. B. Danilov, P. N. Dashuk, S. A. Tul'skii, L. L. Chelnokov, and I. L. Yachnev, Sov. Phys. Tech. Phys. 24, 907 (1979).
9. O. B. Danilov, A. P. Zhevlakov, S. A. Tul'skii, and I. L. Yachnev, Sov. J. Quantum Electron. 12, 786 (1982).
10. S. I. Andreev, I. M. Belousova, P. N. Dashuk, D. Yu. Zaroslov, E. A. Zobov, N. V. Karlov, G. P. Kuz'min, S. M. Nikiforov, A. M. Prokhorov, A. N. Sidorov, L. L. Chelnokov, and M. D. Yarysheva, JETP Lett. 21, 194 (1975).
11. S. I. Andreev, I. M. Belousova, P. N. Dashuk, D. Yu. Zaroslov, E. A. Zobov, N. V. Karlov, G. P. Kuz'min, S. M. Nikiforov, and A. M. Prokhorov, Sov J. Quantum Electron. 6, 931 (1976).
12. D. Yu. Zaroslov, N. V. Karlov, G. P. Kuz'min, and S. M. Nikiforov, Sov. J. Quantum Electron. 8, 695 (1978).
13. A. E. Belyanko, N. I. Lipatov, P. P. Pashinin, and A. M. Prokhorov, J. Phys. (Paris) 40, C7-505 (1979).
14. D. Yu. Zaroslov, N. V. Karlov, G. P. Kuz'min, D. McKen, S. M. Nikiforov, and A. M. Prokhorov, Bull. Acad. Sci. USSR (Phys.) 43, 5 (1979) [Izv. Akad. Nauk SSSR Ser. Fiz. 43, 230 (1979)].
15. D. Yu. Zaroslov, N. V. Karlov, G. P. Kuz'min, and D. McKen, Sov. J. Quantum Electron. 8, 1048 (1978).
16. Yu. I. Bychkov, D. Yu. Zaroslov, N. V. Karlov, G. P. Kuz'min, V. V. Osipov, A. M. Prokhorov, and V. A. Tel'nov, Sov. J. Quantum Electron. 12, 1105 (1982).
17. E. P. Bel'kov, P. N. Dashuk, and G. L. Spichkin, Sov. Phys. Tech. Phys. 27, 1216 (1982).
18. G. V. Eremenko, D. Yu. Zaroslov, N. V. Karlov, I. O. Kovalev, G. P. Kuz'min, and A. M. Prokhorov, Sov. J. Quantum Electron. 13, 996 (1983).
19. P. A. Atanasov, D. Yu. Zaroslov, N. V. Karlov, I. O. Kovalev, G. P. Kuz'min, and A. M. Prokhorov, Sov. Tech. Phys. Lett. 9, 400 (1983).
20. Yu. I. Bychkov, D. Yu. Zaroslov, N. V. Karlov, G. P. Kuz'min, G. A. Mesyats, V. V. Osipov, A. M. Prokhorov, and V. A. Tel'nov, Sov. Phys. Tech. Phys. 28, 916 and 1309 (1983).
21. M. N. Kostin, V. F. Tarasenko, and A. I. Fedorov, Sov. Phys. Tech. Phys. 25, 704 (1980).
22. V. Yu. Baranov, V. M. Borisov, A. M. Davidovskii, and O. B. Khristoforov, Sov. J. Quantum Electron. 11, 42 (1981).
23. V. Yu. Baranov, V. M. Borisov, and O. B. Khristoforov, Sov. J. Quantum Electron. 11, 93 (1981).
24. A. S. Bashkin, P. G. Grigor'ev, A. N. Oraevskii, and A. B. Skvortsov, Sov. J. Quantum Electron. 6, 994 (1976).
25. N. G. Basov, A. S. Bashkin, P. G. Grigor'ev, A. N. Oraevskii, and O. E. Porodinkov, Sov. J. Quantum Electron. 6, 1128 (1976).
26. P. N. Dashuk, Yu. A. Rymarchuk, V. M. Fomin, and L. L. Chelnokov, Sov. Tech. Phys. Lett. 8, 525 (1982).
27. V. M. Borisov, A. M. Davidovskii, and O. B. Khristoforov, Sov. J. Quantum Electron. 12, 1403 (1982).
28. V. M. Borisov, F. I. Vysikailo, Yu. B. Kiryukhin, and O. B. Khristoforov, Sov. J. Quantum Electron. 13, 1408 (1983).
29. K. Watanabe, Y. Sato, M. Obara, and T. Fujioka, Japn. J. Appl. Phys. 19, 2175 (1980).
30. H. Hokazono, K. Hishinuma, K. Watanabe, M. Obara, and T. Fujioka, J. Appl. Phys. 53, 1359 (1982).
31. R. E. Beverly III, Proc. Fifth Int. Sym. Gas Flow Chem. Lasers (Oxford, 20-24 Aug. 1984) (in press).

END

FILMED

12-85

DTIC